International Journal of Multiphysics
Volume 20, No. 1, 2026
ISSN: 1750-9548

# First-Principles Investigation of Half-Metallic Ferromagnetism in Fe- and Mn-Doped CdN and ZnN for Spintronic Applications

**Lalnunpuia[1], Lalmuanawma Chhangte[2,*], T Malsawmtluanga[2], Lalrintluanga Sailo[3], Remlalsiama[3], Lawrence Zonunmawia[3], Zaithanzauva Pachuau[4], Malsawmtluanga[5], Ricky Lalhmangaihzuala[6]**

[1]Department of Physics, Govt. Champhai College, Champhai, Mizoram, India

[2]Department of Physics, Lunglei Govt. College, Lunglei, Mizoram, India

[3]Department of Physics, Govt. Zirtiri Res. Sc. College, Aizawl, Mizoram, India

[4]Department of Physics, Mizoram University, Aizawl, Mizoram, India

[5]Research Scholar, Mizoram University, Aizawl, Mizoram, India

[6]Department of Physics, Govt. Zirtiri Res. Sc. College, Aizawl, Mizoram, India

[*]Corresponding Author: muana.chhangte@gmail.com

***Abstract:***

The modification of electronic and magnetic properties of CdN and ZnN through transition metal doping is explored using first-principles calculations based on density functional theory. Fe and Mn atoms were introduced at a concentration of 37.5% within a supercell framework, and their influence on the host materials was systematically analyzed. The results indicate that doping significantly alters the electronic structure, leading to spin-dependent band formation. Fe incorporation promotes a clear separation between spin channels, resulting in half-metallic behavior in both CdN and ZnN. Mn doping produces a similar effect in ZnN, while CdN remains predominantly metallic with enhanced spin asymmetry. The observed behavior is driven by hybridization between transition metal d-states and nitrogen p-states, which induces exchange splitting near the Fermi level. High spin polarization values suggest that these doped nitrides may serve as potential materials for spin-dependent transport applications.

***Keywords:*** First-principles calculations; Half-metallic ferromagnetism; Transition metal doping; CdN and ZnN; Spin polarization

## 1. Introduction

The increasing demand for high-performance and energy-efficient electronic devices has led to the rapid development of spintronics, where both the charge and spin of electrons are utilized for information processing. In this context, materials capable of generating highly spin-polarized currents are of great importance for applications such as spin valves, magnetic tunnel junctions, and spin injectors. Half-metallic ferromagnets represent a unique class of materials that exhibit metallic behavior in one spin channel and semiconducting or insulating behavior in the other, resulting in 100% spin polarization at the Fermi level [1,2].

One of the most promising approaches to achieve such properties is through the formation of dilute magnetic semiconductors by doping non-magnetic host materials with transition metal elements. The introduction of transition metal atoms gives rise to localized *d*-electron states, which interact with the host lattice via *p*-*d* hybridization, leading to exchange splitting and magnetic ordering [3]. The strength of these interactions determines the extent of spin polarization and the possibility of achieving half-metallicity.

Binary nitrides such as CdN and ZnN have emerged as potential host materials due to their structural stability and tunable electronic properties. ZnN is generally reported as a semiconductor with a moderate band

gap, while CdN lies close to a semi metallic regime, making it highly responsive to doping-induced modifications [4-6]. These characteristics make both compounds suitable candidates for exploring spin-dependent electronic behavior.

Among various transition metal dopants, Iron (Fe) and Manganese (Mn) are of particular interest due to their partially filled 3*d* orbitals and strong exchange interactions. When incorporated into CdN and ZnN, these dopants can significantly alter the electronic structure near the Fermi level. The hybridization between transition metal d-states and nitrogen p-states leads to the formation of spin-dependent bands, which can result in half-metallic ferromagnetism under appropriate conditions [7,8].

From a theoretical perspective, density functional theory (DFT) has proven to be an effective tool for investigating the electronic and magnetic properties of such systems. First-principles calculations based on DFT enable a detailed understanding of band structure, density of states, and magnetic interactions at the atomic level [9,10].

In this work, a comprehensive first-principles study is carried out to investigate the electronic structure, density of states, spin polarization, and magnetic properties of Fe- and Mn-doped CdN and ZnN at a doping concentration of 37.5%. Particular attention is given to the role of *p-d* hybridization and exchange splitting in determining half-metallic behavior. The findings provide valuable insight into the design of transition metal doped nitrides for potential spintronic applications.

## 2. Computational Methodology

The electronic and magnetic properties of Fe- and Mn-doped CdN and ZnN were investigated using density functional theory (DFT) [9,10]. All calculations were performed employing the full-potential linearized augmented plane wave (FP-LAPW) method, as implemented in the WIEN2k simulation package [11-13]. This approach provides an accurate description of the electronic structure without introducing shape approximations to the potential or charge density.

The exchange–correlation effects were treated within the generalized gradient approximation (GGA) using the Perdew-Burke-Ernzerhof (PBE) functional [14-16]. Within the FP-LAPW framework, the crystal is divided into non-overlapping muffin-tin spheres and an interstitial region. The wave functions inside the atomic spheres were expanded up to a maximum angular momentum quantum number of $l_{max}$ = 10, while plane waves were used to describe the interstitial region.

The basis set size was controlled by the parameter $R_{MT}\times K_{max}$, which was fixed at 7.0, ensuring a reliable balance between computational accuracy and efficiency. Brillouin zone integrations were carried out using a Monkhorst-Pack *k*-point mesh consisting of 63 *k*-points [17]. The self-consistent field (SCF) calculations were considered converged when the total energy difference between successive iterations was less than $10^{-4}$ Ry.

The parent compounds CdN and ZnN crystallize in the cubic rock salt structure (space group $Fm\bar{3}m$). The equilibrium lattice parameters were taken as 4.72 Å for CdN and 4.50 Å for ZnN . To model the effect of doping, 2×2×2 supercells containing eight formula units were constructed. Transition metal atoms (Fe and Mn) were substituted at the cation sites, corresponding to a doping concentration of 37.5%, resulting in compositions $Cd_{0.625}Fe_{0.375}N$, $Cd_{0.625}Mn_{0.375}N$, $Zn_{0.625}Fe_{0.375}N$, and $Zn_{0.625}Mn_{0.375}N$.

The muffin-tin radii ($R_{MT}$) were carefully selected to avoid overlap between neighboring spheres while ensuring accurate representation of the basis functions. The chosen values were 1.52 Å for Cd, 1.37 Å for Zn, 1.26 Å for Fe and Mn, and 0.74 Å for nitrogen. All calculations were performed within a spin-polarized framework to capture the magnetic interactions induced by transition metal doping.

## 3. Results and Discussion

### 3.1. Structure and Volume Optimization

The structural response of Fe- and Mn-doped CdN and ZnN was examined through total energy calculations performed over a series of unit cell volumes. The systems were modeled within a cubic rock salt

framework, where transition metal atoms substitute cation sites in a 2×2×2 supercell, corresponding to a doping concentration of 37.5%. This configuration allows for a realistic description of substitutional doping while preserving the overall crystal symmetry.

The equilibrium structural parameters were obtained by fitting the calculated energy-volume data to the third-order Birch–Murnaghan equation of state [18], which provides a reliable description of the elastic behavior of solids under isotropic compression:

$$E(V) = E_0 + \frac{9V_0B_0}{16}\left[\left\{\left(\frac{V_0}{V}\right)^{2/3} - 1\right\}^3 B_0' + \left\{\left(\frac{V_0}{V}\right)^{2/3} - 1\right\}^2 \left\{6 - 4\left(\frac{V_0}{V}\right)^{2/3}\right\}\right]$$

where $E_0$, $V_0$, $B_0$ and $B_0'$ represent the equilibrium energy, equilibrium volume, bulk modulus and its pressure derivative respectively. The fitted curves allow accurate identification of the ground-state structural parameters.

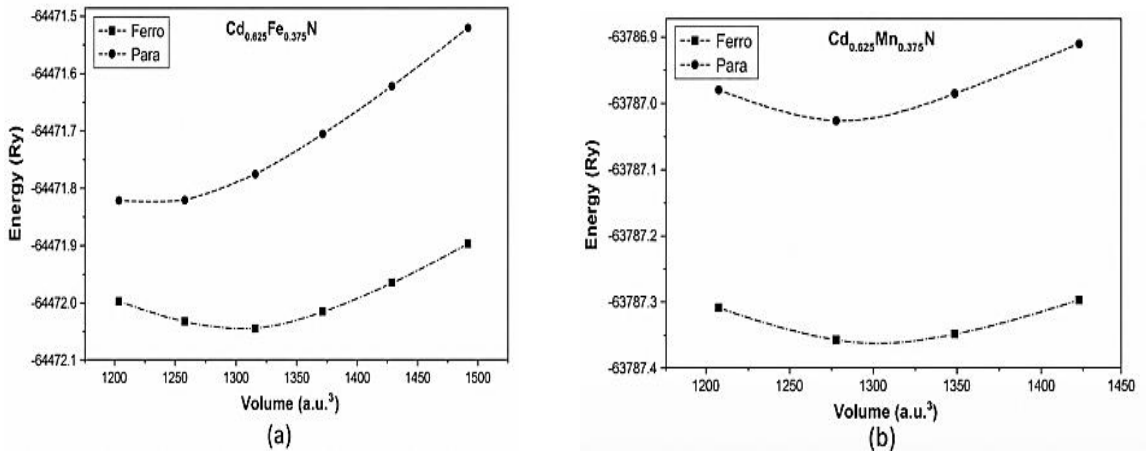


**Fig. 1. Total energy as a function of volume for Cd-based doped compounds: (a) $Cd_{0.625}Fe_{0.375}N$ and (b) $Cd_{0.625}Mn_{0.375}N$, calculated within the GGA approximation.**

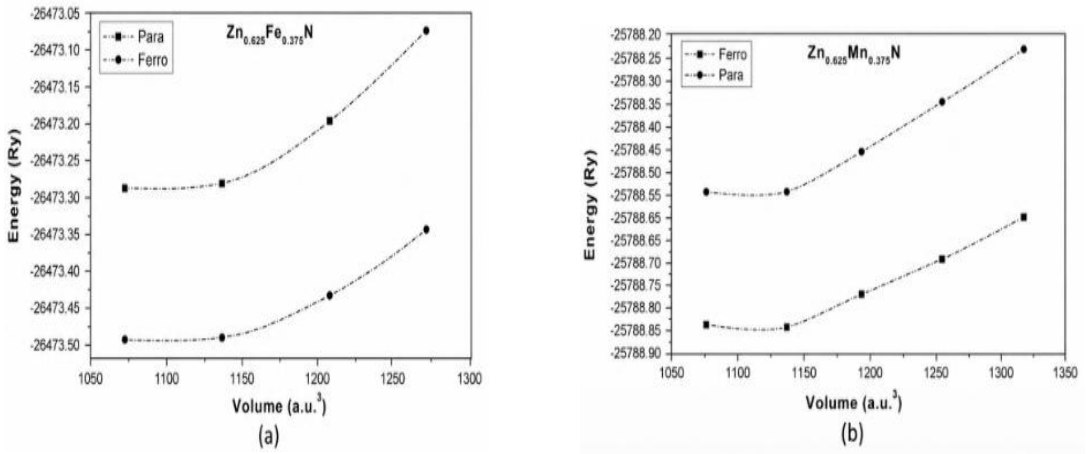


**Fig. 2. Total energy as a function of volume for Zn-based doped compounds: (a) $Zn_{0.625}Fe_{0.375}N$ and (b) $Zn_{0.625}Mn_{0.375}N$, calculated within the GGA approximation.**

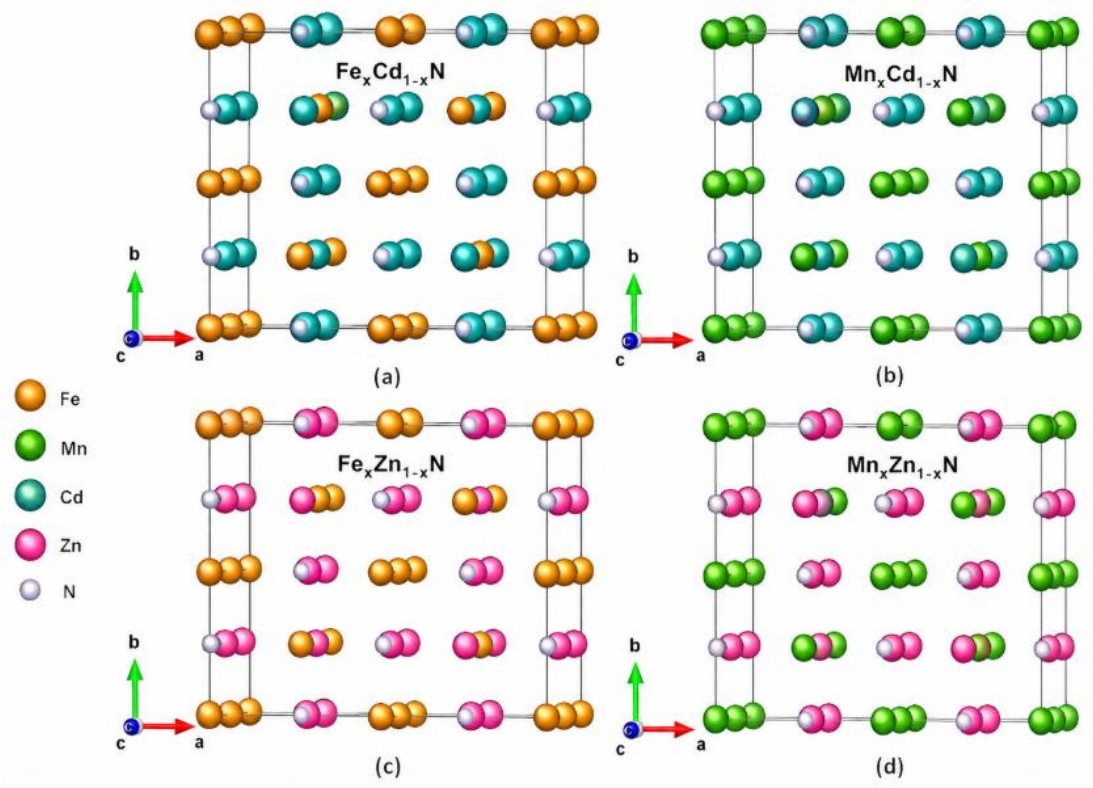


**Fig. 3. Crystal structures of (a) $Cd_{0.625}Fe_{0.375}N$, (b) $Cd_{0.625}Mn_{0.375}N$, (c) $Zn_{0.625}Fe_{0.375}N$, and (d) $Zn_{0.625}Mn_{0.375}N$ showing substitutional positions of transition metal atoms in the rock salt lattice.**

The resulting energy–volume profiles for Fe-doped compounds (Fig. 1) and Mn-doped compounds (Fig. 2) display distinct minima, confirming that all configurations reach stable equilibrium states. The smooth variation of energy with volume indicates that the crystal lattice remains well-behaved under compression and expansion. In addition, the ferromagnetic configuration is consistently found to be energetically more favorable than the non-magnetic state, suggesting that magnetic ordering is intrinsically linked to structural stability in these systems.

A comparison of optimized lattice parameters shows only marginal deviations from the corresponding undoped compounds. This indicates that the substitution of Cd and Zn atoms by Fe and Mn does not introduce significant lattice strain, despite differences in atomic radii and electronic configurations. Such behavior reflects the compatibility of transition metal dopants with the host lattice.

The relaxed atomic structures, illustrated in Fig. 3, confirm that Fe and Mn atoms occupy substitutional positions within the cation sublattice. No observable symmetry breaking or structural distortion is detected after relaxation, demonstrating that the cubic phase is preserved upon doping. The local atomic environment remains nearly symmetric, with only minor adjustments in bond lengths around the dopant sites.

From a physical perspective, maintaining structural integrity is essential for preserving the electronic interactions responsible for magnetic behavior. The stability of the doped lattice ensures consistent overlap between transition metal *d*-states and nitrogen *p*-states, which plays a key role in exchange splitting and spin polarization. Therefore, the optimized structures obtained in this section provide a reliable foundation for the electronic and magnetic analyses presented in the subsequent sections.

### 3.2 Density of States (DOS)

The electronic behavior of Fe- and Mn-doped CdN and ZnN was analyzed through spin-resolved density of states calculations, as presented in Fig. 4. The DOS profiles provide insight into the distribution of electronic states near the Fermi level and the origin of spin-dependent conductivity in these systems.

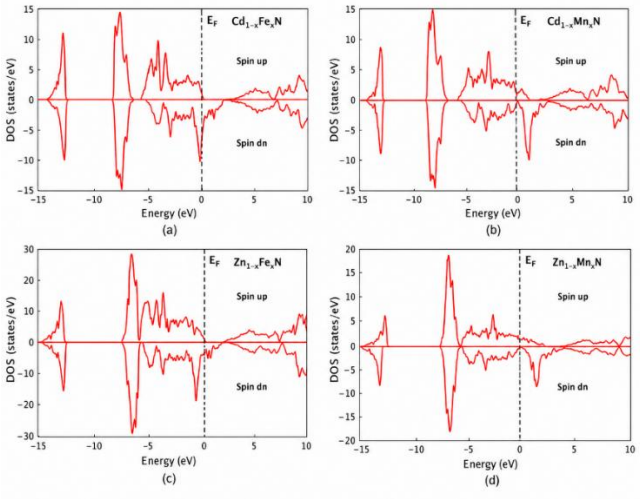


**Fig. 4. Total density of states (DOS) of (a) $Cd_{0.625}Fe_{0.375}N$, (b) $Cd_{0.625}Mn_{0.375}N$, (c) $Zn_{0.625}Fe_{0.375}N$, and (d) $Zn_{0.625}Mn_{0.375}N$ for spin-up and spin-down channels.**

For $Cd_{0.625}Fe_{0.375}N$, the DOS shows a clear asymmetry between spin channels. The majority spin (spin-up) exhibits finite states at the Fermi level, indicating metallic behavior, whereas the minority spin (spin-down) displays a distinct energy gap. This confirms the half-metallic character of the compound. The PDOS in Fig. 5 reveals that this behavior originates from strong hybridization between Fe-3d states and N-2p states, which leads to exchange splitting of the d-orbitals.

In $Cd_{0.625}Mn_{0.375}N$, both spin channels show states crossing the Fermi level, indicating metallic behavior. Although a noticeable difference in the density of states between spin-up and spin-down channels is observed, the absence of a band gap in either channel suggests that the system does not exhibit half-metallicity. The Mn-3d states are more broadly distributed around the Fermi level, resulting in weaker spin-dependent separation.

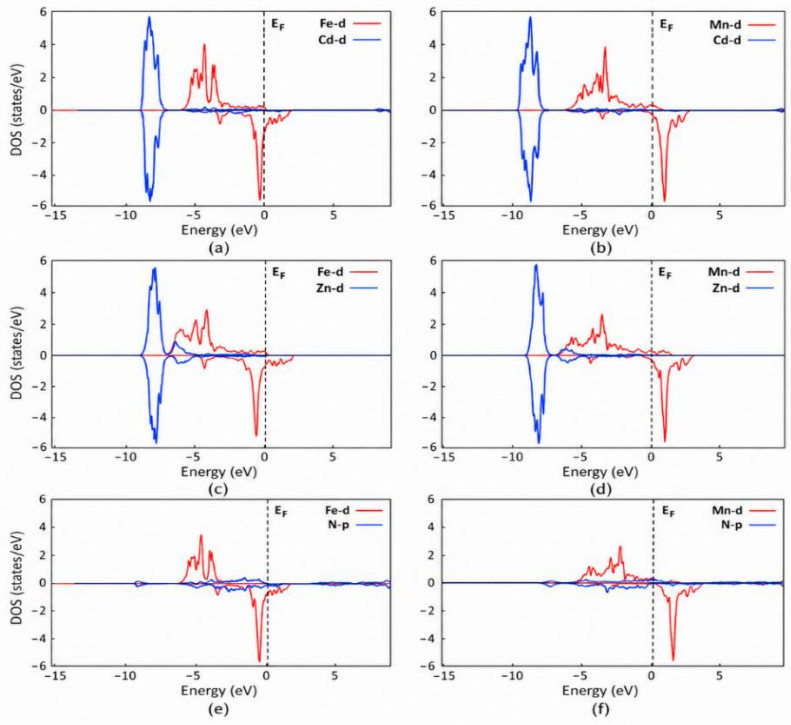


**Fig. 5. Partial density of states (PDOS) showing the contributions of transition metal 3d states and N-2p states for the doped compounds.**

A different trend is observed in Zn-based compounds. For $Zn_{0.625}Fe_{0.375}N$, the spin-up channel remains metallic, while a gap appears in the spin-down channel, confirming half-metallic behavior similar to the Cd-based Fe-doped system. In $Zn_{0.625}Mn_{0.375}N$, a well-defined gap is observed in the minority spin channel, indicating half-metallicity. This suggests that Mn doping is more effective in inducing half-metallic behavior in ZnN than in CdN.

The DOS analysis highlights that the emergence of half-metallicity is strongly dependent on both the dopant and the host lattice. The interaction between transition metal d-states and nitrogen p-states plays a key role in determining the spin-dependent electronic structure.

### 3.3 Band Structure

The spin-resolved band structures shown in Fig. 6 and Fig. 7 provide a detailed picture of the electronic dispersion and confirm the trends observed in the DOS analysis.

For $Cd_{0.625}Fe_{0.375}N$ (Fig. 6a–b), the spin-up bands clearly cross the Fermi level along several high-symmetry directions, indicating metallic behavior. In contrast, the spin-down channel shows a significant reduction of band crossings near the Fermi level, with an apparent gap-like region forming around it. This supports the presence of strong spin polarization and near half-metallic behavior.

In $Cd_{0.625}Mn_{0.375}N$ (Fig. 6c–d), both spin-up and spin-down bands intersect the Fermi level, confirming metallic behavior in both channels. The absence of a band gap in the minority spin channel indicates that the compound does not exhibit half-metallicity.

The band structures for Zn-based compounds (Fig. 7) show a different trend. For $Zn_{0.625}Fe_{0.375}N$ (Fig. 7a–b), the spin-up channel remains metallic, while the spin-down channel exhibits fewer band crossings near the Fermi level, indicating enhanced spin splitting. In $Zn_{0.625}Mn_{0.375}N$ (Fig. 7c–d), the spin-down channel shows a clear gap around the Fermi level, confirming half-metallic behavior, whereas the spin-up channel remains metallic.

The differences observed between Fe and Mn doping can be attributed to the relative position and occupancy of the 3*d* orbitals. Fe induces stronger exchange splitting, while Mn leads to broader band dispersion. Additionally, the host lattice plays a critical role, with ZnN favoring half-metallicity more strongly than CdN.

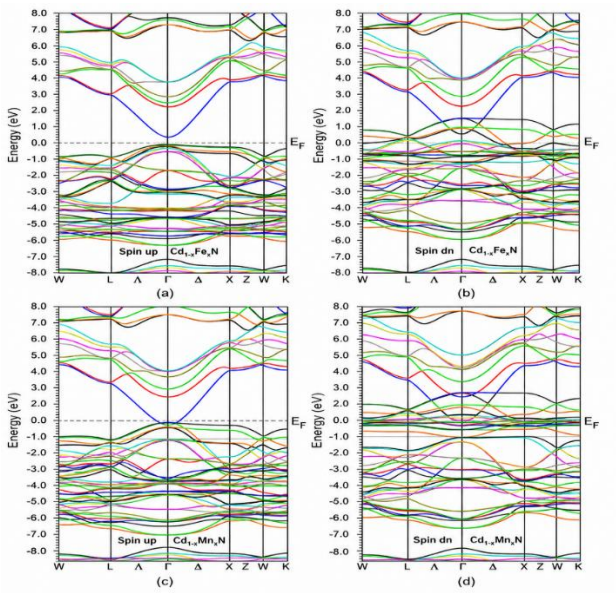


**Fig. 6. Spin-resolved band structure of Cd-based compounds: (a) spin-up and (b) spin-down for $Cd_{0.625}Fe_{0.375}N$, and (c) spin-up and (d) spin-down for $Cd_{0.625}Mn_{0.375}N$.**

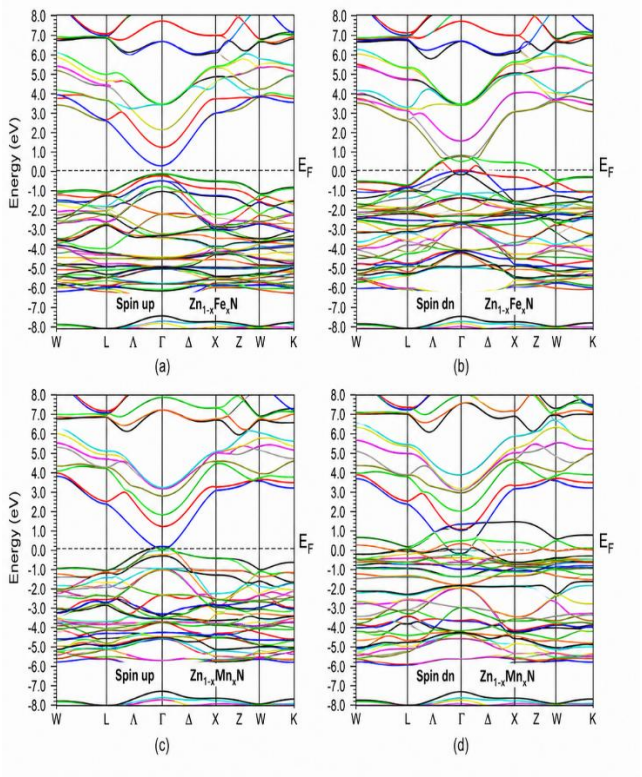


**Fig. 7. Spin-resolved band structure of Zn-based compounds: (a) spin-up and (b) spin-down for $Zn_{0.625}Fe_{0.375}N$, and (c) spin-up and (d) spin-down for $Zn_{0.625}Mn_{0.375}N$.**

### 3.4 Magnetic Properties

The magnetic characteristics of Fe- and Mn-doped CdN and ZnN were investigated using spin-polarized first-principles calculations. The substitution of transition metal atoms at cation sites induces magnetic ordering through exchange interactions between localized d-electrons and the surrounding nitrogen atoms.

To provide a unified view of the electronic and magnetic behavior, the calculated total magnetic moments and spin polarization values are summarized in Table 1.

**Table 1. Magnetic moments and spin polarization of doped CdN and ZnN**

| Compound | Magnetic Moment (μB) | Spin Polarization (%) |
|---|---|---|
| $Cd_{0.625}Fe_{0.375}N$ | 6.00 | 100 |
| $Cd_{0.625}Mn_{0.375}N$ | 5.00 | ~60 |
| $Zn_{0.625}Fe_{0.375}N$ | 4.00 | ~90 |
| $Zn_{0.625}Mn_{0.375}N$ | 5.00 | 100 |

The results show that all doped systems possess finite magnetic moments, confirming the emergence of ferromagnetism. The dominant contribution to the magnetic moment originates from the transition metal 3*d* orbitals, while nitrogen atoms contribute weakly through induced polarization.

For Fe-doped systems, the magnetic moments are influenced by the partially filled Fe-3*d* orbitals, which exhibit strong exchange splitting. $Cd_{0.625}Fe_{0.375}N$ shows the highest magnetic moment due to stronger localization and reduced hybridization compared to the Zn-based counterpart. In $Zn_{0.625}Fe_{0.375}N$, the slightly lower magnetic moment reflects increased hybridization between Fe-3*d* and N-2*p* states.

In Mn-doped compounds, the magnetic moments are governed by the half-filled d-shell configuration of Mn, leading to stable high-spin states. Both $Cd_{0.625}Mn_{0.375}N$ and $Zn_{0.625}Mn_{0.375}N$ exhibit magnetic moments close to 5 μB, consistent with Hund's rule coupling. The integer nature of magnetic moments observed in several compounds indicates a strong correlation between electronic structure and magnetic ordering, which is often associated with half-metallic systems.

### 3.5 Spin Polarization

Spin polarization at the Fermi level is a key parameter for evaluating the suitability of materials for spintronic applications. It is defined as:

$$P = \frac{N\left(E_F^{\uparrow}\right) - N\left(E_F^{\downarrow}\right)}{N\left(E_F^{\uparrow}\right) + N\left(E_F^{\downarrow}\right)}$$

where $N\left(E_F^{\uparrow}\right)$ and $N\left(E_F^{\downarrow}\right)$ represent the density of states at the Fermi level for spin-up and spin-down channels, respectively.

For $Cd_{0.625}Fe_{0.375}N$ and $Zn_{0.625}Mn_{0.375}N$, the complete absence of states at the Fermi level in the minority spin channel leads to 100% spin polarization, confirming their half-metallic nature. In $Zn_{0.625}Fe_{0.375}N$, a high but incomplete spin polarization (~90%) is observed due to residual states in the minority spin channel. In contrast, $Cd_{0.625}Mn_{0.375}N$ exhibits partial spin polarization (~60%), as both spin channels contribute states at the Fermi level. This behavior is consistent with its metallic band structure.

The variation in spin polarization can be understood in terms of exchange splitting and p–d hybridization. Stronger exchange interaction leads to a larger separation between spin channels, resulting in higher spin polarization. This explains why Fe doping and Mn doping in ZnN favor half-metallicity, while Mn doping in CdN does not.

These results indicate that the combination of high magnetic moment and high spin polarization makes Fe-doped CdN and Mn-doped ZnN particularly promising for spin injection and spin filtering applications.

## 4. Conclusions

A systematic first-principles investigation of Fe- and Mn-doped CdN and ZnN has been carried out to understand their structural, electronic, and magnetic properties. The structural analysis confirms that all doped compounds remain stable in the cubic rock salt phase, with only minor changes in lattice parameters upon substitution. The electronic structure results reveal a strong dependence on both the dopant and host lattice. Fe doping induces pronounced spin asymmetry in both CdN and ZnN, leading to nearly half-metallic behavior, while Mn doping results in half-metallicity only in ZnN, with $Cd_{0.625}Mn_{0.375}N$ retaining metallic character.

The magnetic calculations show that all systems exhibit ferromagnetic ordering, with magnetic moments primarily originating from transition metal 3d states. Mn-doped systems display moments close to high-spin configurations, whereas Fe-doped systems show enhanced hybridization effects. The calculated spin polarization further confirms that $Cd_{0.625}Fe_{0.375}N$ and $Zn_{0.625}Mn_{0.375}N$ achieve nearly complete spin polarization, highlighting their half-metallic nature.

Overall, the results demonstrate that selective doping and host choice play a critical role in tailoring spin-dependent properties. In particular, Fe-doped CdN and Mn-doped ZnN emerge as promising candidates for spintronic applications requiring high spin polarization and stable ferromagnetism.

## References

[1] Žutić, I., Fabian, J., Das Sarma, S. Spintronics: Fundamentals and applications. *Rev. Mod. Phys*. 76 (2004) 323–410.

https://doi.org/10.1103/RevModPhys.76.323

[2] Katsnelson, M.I., Irkhin, V.Y., Chioncel, L., Lichtenstein, A.I., de Groot, R.A. Half-metallic ferromagnets: From band structure to many-body effects. *Rev. Mod. Phys*. 80 (2008) 315–378.

https://doi.org/10.1103/RevModPhys.80.315

[3] Dietl, T., Ohno, H., Matsukura, F. Ferromagnetism in dilute magnetic semiconductors. *Science* 287 (2000) 1019–1022.

https://doi.org/10.1126/science.287.5455.1019

[4] Jiang, X., et al. Optical properties of $Zn_3N_2$ thin films. *J. Appl. Phys*. 111 (2012) 033709.

https://doi.org/10.1063/1.3681296

[5] Zong, F., et al. Structural and optical properties of $Zn_3N_2$ films. J. *Phys. D: Appl. Phys*. 39 (2006) 3051–3055.

https://doi.org/10.1088/0022-3727/39/14/023

[6] Zhao, Y., et al. Electronic properties of CdN: First-principles study. *Physica B* 405 (2010) 4522–4525.

https://doi.org/10.1016/j.physb.2010.08.022

[7] Sato, K., Katayama-Yoshida, H. First-principles design of magnetic semiconductors. Semicond. *Sci. Technol.* 17 (2002) 367–376.

https://doi.org/10.1088/0268-1242/17/4/304

[8] de Groot, R.A., et al. Half-metallic ferromagnets. *Phys. Rev. Lett.* 50 (1983) 2024–2027.

https://doi.org/10.1103/PhysRevLett.50.2024

[9] Hohenberg, P., Kohn, W. Inhomogeneous electron gas. *Phys. Rev.* 136 (1964) B864–B871.

https://doi.org/10.1103/PhysRev.136.B864

[10] Kohn, W., Sham, L.J. Self-consistent equations including exchange and correlation effects. *Phys. Rev.* 140 (1965) A1133–A1138.

https://doi.org/10.1103/PhysRev.140.A1133

[11] Blaha, P., Schwarz, K., Madsen, G.K.H., Kvasnicka, D., Luitz, J. WIEN2k: An augmented plane wave + local orbitals program for calculating crystal properties, Vienna University of Technology (2001).

[12] Madsen, G.K.H., Blaha, P., Schwarz, K., Sjöstedt, E., Nordström, L. Efficient linearization of the augmented plane-wave method. *Phys. Rev. B* 64 (2001) 195134.

https://doi.org/10.1103/PhysRevB.64.195134

[13] Schwarz, K., Blaha, P., Madsen, G.K.H. Electronic structure calculations of solids using WIEN2k. Comput. Phys. Commun. 147 (2002) 71–76.

https://doi.org/10.1016/S0010-4655(02)00206-0

[14] Perdew, J.P., Zunger, A. Self-interaction correction to density-functional approximations. *Phys. Rev. B* 23 (1981) 5048–5079.

https://doi.org/10.1103/PhysRevB.23.5048

[15] Perdew, J.P., Burke, K., Ernzerhof, M. Generalized gradient approximation made simple. *Phys. Rev. Lett*. 77 (1996) 3865–3868.

https://doi.org/10.1103/PhysRevLett.77.3865

[16] Perdew, J.P., Burke, K., Ernzerhof, M. Generalized gradient approximation (Erratum). *Phys. Rev. Lett.*

78 (1997) 1396.

https://doi.org/10.1103/PhysRevLett.78.1396

[17] Monkhorst, H.J., Pack, J.D. Special points for Brillouin-zone integrations. *Phys. Rev. B* 13 (1976) 5188–5192.

https://doi.org/10.1103/PhysRevB.13.5188

[18] Birch, F. Finite elastic strain of cubic crystals. *Physical Review* 71 (1947) 809–824. https://doi.org/10.1103/PhysRev.71.809

[19] [19] Sato, K., Katayama-Yoshida, H. First-principles materials design for semiconductor spintronics. *Semicond. Sci. Technol.* 17 (2002) 367–376.

https://doi.org/10.1088/0268-1242/17/4/304

[20] de Groot, R.A., et al. New class of materials: Half-metallic ferromagnets. *Phys. Rev. Lett.* 50 (1983) 2024–2027.
https://doi.org/10.1103/PhysRevLett.50.2024